

A Novel Hybrid Actuator for The Hand Exoskeleton

Jianyu Yang, Tao Wei, Hui Shi

Abstract— As a new type of intelligent material, shape memory alloy (SMA) has been gradually applied to robot actuators due to its unique shape memory effect. However, the existing SMA actuators generally have slow response and high energy consumption. In this paper, a novel hybrid actuator and its control method based on shape memory alloy (SMA) are proposed for a bidirectional coupling hand exoskeleton actuator. Compared with the traditional two-way SMA actuator, this paper uses a two-way hybrid actuator combining SMA springs with servo motors, which integrated the advantages of servo motor and SMA. The compact actuator can ensure rapid response and force control at the target location, and is more secure.

I. INTRODUCTION

Due to the aging of the population and the threat of diseases such as stroke, people are in urgent need of equipment that can assist human to complete or enhance the physical movement ability and complete rehabilitation training in daily life. Physical rehabilitation is essential for the treatment of patients with physical or neurological disabilities [1]. As a kind of intelligent device that imitates the physiological structure of human body and can be worn by human beings, the exoskeleton robot can cooperate with the wearer's movement and assist the wearer at the same time, which has attracted more and more scholars' attention. In recent ten years, the hand exoskeleton has developed rapidly. Marco Cempini [2] and Hu Huang [3] et al. designed the hand exoskeleton actuator by motor and tendon. Ma Zhuo [4] and Gazi Akgun [5] et al. used servo motor to directly

actuator the hand exoskeleton. Although the response was fast, the impact was large, and the exoskeleton movement did not conform to the movement rules of human hands. Yaxi Wang [6] designed a pneumatic robot. Benjamin W.K. Ang [7], et al. proposed a 3D printing to make pneumatic gloves for hand rehabilitation, requiring high air tightness. Filomena [8] has designed an SMA-actuator dexterous hand that enables good hand movement. Namseon Jang [9] has designed a surgical device using an SMA memory alloy with high safety and precision. Feng Xiaobin [10] proposed a two-way symmetrical memory alloy-actuator hand exoskeleton, the stability of motion has been improved, but the response is slow, it is difficult to achieve real-time motion control.

In view of the above problems, a hybrid actuator and control method based on SMA spring are proposed on the basis of the work of the pre-bidirectional motion coupling tendon scheme. The second section of this paper introduces the power system structure design and system hardware. The third section establishes the control model applicable to the two-way coupling scheme. The fourth section and five sections are the experimental analysis and conclusion respectively.

II. MECHANICAL STRUCTURE AND HARDWARE ARCHITECTURE OF HAND EXOSKELETON

In the previous work, our team proposed a two-way coupling finger tendon arrangement scheme [11] that conforms to the law of human finger movement. Because Main-ext tendon and Main-flex tendon use different materials, tendon actuators are required to achieve the movement characteristics of the two-sided main tendon. In

*Resrach supported by the National Natural Sci-ence Foundation Grant No. 51505072.

All authors are with School of Mechanical Engineering & Automation, Northeastern University, Shenyang 110819, China.

*Contacting Author: Jianyu Yang is with School of Mechanical Engineering & Automation, Northeastern University, Shenyang 110819, China. (email: jyyang@mail.neu.edu.cn)

this paper, a power system scheme conforming to the law of human movement is proposed, as shown in Fig. 1, including the end finger execution part, the palm-side shape memory alloy actuator part, the back motor actuator part and the controller part. The coupling tendon fixed to the finger part is actuated by a back-side motor-actuator tendon winch to achieve finger stretching movement, and the palm side SMA spring actuates the tendon fixed to the palm of the finger to achieve stable finger bending movement. There are two main reasons for using a symmetrical hybrid actuator:

- A. Compact and easy to control. For wearable hand exoskeleton devices, too large drive motor leads to bulky system, while small drive motor is underpowered. Nitino SMA springs have a clear advantage because they are easier to heat and produce sufficient force while maintaining overall structural compactness.
- B. Faster response and high security. The response time of the Nitino SMA spring is slightly slower than that of the servo motor actuator, which can be slowed if the same Nitino SMA spring actuator is used on both sides of the hand. Because the Nickelodeon SMA spring itself has a good stretch, so that when the Nickelodeon SMA spring as a power source, the grasping of the exoskeleton of the hand is better, in line with the movement law of the hand, high safety.

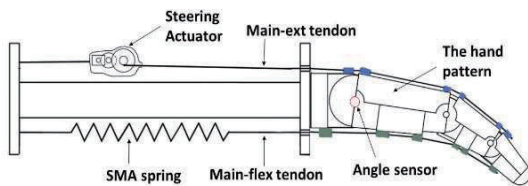


Figure 1. Hybrid drive system

In this paper, the MG996R Steering Actuator is selected instead of the motor-winch mechanism, the model actuator is compact, the power weight is relatively high, 55g actuator can provide a maximum torque of 13Kg. The steering actuator, which serves as a servo actuator with a rotation range of -90 to 90 degrees, enables real-time and accurate motion position control and ensures fast finger

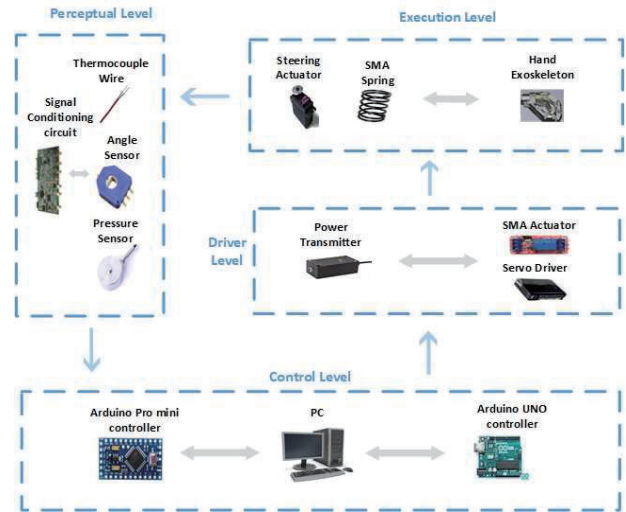


Figure 2. Hardware system of hand exoskeleton

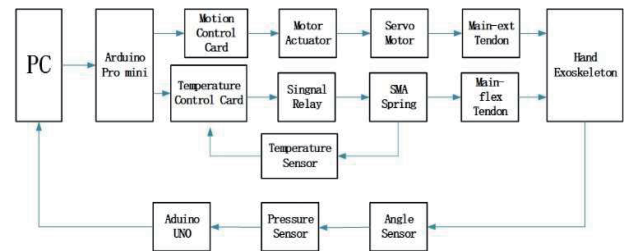


Figure 3. Overall control diagram of the hand exoskeleton

stretching without load. The SMA spring with one-way memory effect is selected, the original length and maximum re-deformation of the spring are 5mm, and the maximum extrusion is 113.2mm to meet the deformation of the hand tendon. The hardware system of the exoskeleton of the hand, as shown in Fig. 2, consists of four parts: the driver layer, the control layer, the actuator layer and the executive layer, forming a good information interaction. During the operation, the temperature sensor consisting of TT-K-30-1000-SLE thermocouple wire arranged at the spring achieves the temperature monitoring of the SMA spring, and the angle sensor of the finger joint is obtained by the Muada SV01A103CEA01R000 angle sensor arranged on the finger MCP joint. The hand exoskeleton is compacted by a well-arranged sensor unit, providing real-time information for the movement control of the exoskeleton.

III. CONTROL METHOD

A. Control system infrastructure

Since the hand exoskeleton in this article uses an unsymmetrical hybrid actuator, this requires the control system to be able to achieve parallel motion control, as shown in Fig. 3.

B. Control algorithm

The control flow begins with the perception system obtaining four motion parameters: the target fingertip position (TP), the target fingertip force (TF), the current fingertip position (PP), and the current fingertip force (PF). The obtained motion parameters are compared with the motion parameters completed by the last motion, and the corresponding calculations are performed according to the difference between the target parameters and the current parameters to determine whether to hold the action. If the difference is zero, the last data is used to maintain the action, if the difference is not zero, the controller to achieve the control system's return action, the start target temperature (TT) set to 35 °C, start the target finger angle (TFP) set to 0° .

Correction of the target finger gesture (TFP) value. In order to ensure the safe operation of the exoskeleton system, it is necessary to limit the effective range of TFP (target finger posture). The MCP, PIP, and DIP of the design exoskeleton organs have a range of motion of 60° , 90° , and 57° , respectively, so the minimum value of TFP (LFP) is 0° and the maximum value (MFP) is 207° . If the "TEP" value is entered, the TEP value is corrected to the LFP/MFP value if it is not within the design range.

The calculation of the target temperature (TT). The target temperature (TT) value of the control SMA spring is calculated by the target force (TF) defined by the fingertip and the target position (TP) defined by each finger, so the calculation of the target temperature requires three steps: (1) to convert the TP value to the stretch length of the SMA spring; (2) Convert the TF value to SMA spring stretch force; (3) The TT value is calculated using the SMA stretch force and stretch length values.

- Convert the TP value to the stretch length of the SMA

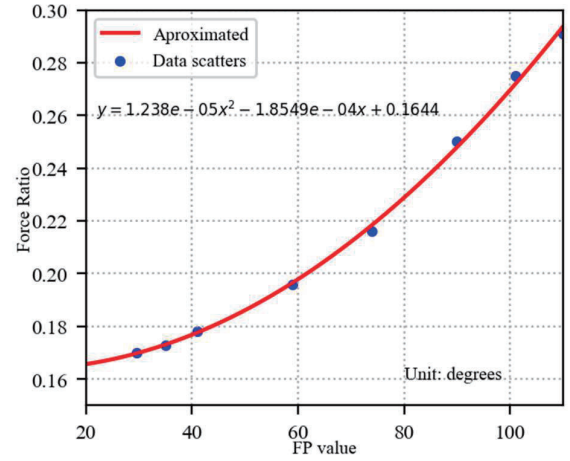


Figure 4. Ratio of the input force on the main flexor tendon to the fingertip output

spring: According to the experimental data of the length of the main driving tendon with the change of finger posture, it can be fitted with the amount of change of main-flex' tendon length, as shown in the equation 1, the α in the pattern is the FP value, i.e. the total angle of the MCP, PIP and DIP joints.

$$\Delta l = -1.1e - 08\alpha^4 + 3.5e - 06\alpha^3 - 2.4e - 04\alpha^2 + 0.21 \quad (1)$$

Since the SMA spring is pre-stretched by 20mm, the total elongity of the SMA spring (target length, L_{tl}) Can be expressed as:

$$L_{tl} = \Delta l + 20 \quad (2)$$

- Convert TF to SMA spring stretch: First of all, the ratio of input force on the main curved tendon to fingertip output force is defined as, K_{ivo} . From the experimental data in [12], K_{ivo} can be obtained, as shown in Fig. 4. And then we can get F_{ts} :

$$K_{ivo} = 1.238e - 05\alpha^2 - 1.855e - 04\alpha + 0.1644 \quad (3)$$

$$F_{ts} = \frac{TF}{K_{ivo}} \quad (4)$$

- Calculate the TT value:
Since the SMA spring actuator is based on ambient temperature changes in memory alloy materials, in order to achieve precise control of the motion of the SMA spring, a thermodynamic analysis of the characteristics of the spring is required, and Table I lists the physical significance of all relevant symbols

used in the thermodynamic analysis. Because the force-displacement equation relationship of the memory alloy SMA spring can be expressed as equation 5, where C_1 and C_2 can be represented by equation 6.

$$C_1(F - F_0) = C_2G(\delta - \delta_0) - C_2\delta_L G(\xi - \xi_0) \quad (5)$$

$$C_1 = \frac{k_s D}{\pi r^3} \quad C_2 = \frac{2r}{\pi D^2 N} \quad (6)$$

TABLE I. Symbols for SMA thermodynamic analysis

Parameter Name	Physical Meanings
A_s/A_f	Austenite start/finish temperature
M_s/M_f	Martensite start/ finish temperature
G_A/G_M	Shear modulus of austenite/ martensite
K_A/K_M	Hook constant of austenite/ martensite
F	Tensile force
F_0	Initial tensile force
G	Shear modulus of any phase state
δ	Tensile displacement
δ_0	Initial tensile displacement
δ_L	Max recoverable tensile displacement
ξ	Martensite volume fraction
ξ_0	Initial martensite volume fraction
k_s	Wahl correction factor
D/r	Average diameter/ radius of the spring
d	Average diameter of the spring wire
N	Number of the coils in the spring
T	Temperature
σ_{eq}	Equivalent stress
τ/σ_{er}	Shear/ Critical stress
σ_e	Elastic limit

As the memory alloy in the phase change process, the material will appear in the martensite and austenite two phase components, so the shear mod G is not a constant, can be calculated using equation 7.

$$G = G_A - \xi(G_A - G_M) \quad (7)$$

The second-order equations of the ξ can be introduced by equations 5 and 7, which ξ the expected equation 9.

$$\begin{cases} D_1 \xi^2 - D_2 \xi + D_3 = 0 \\ D_1 = E \delta_L \\ D_2 = E \delta + G_A \delta_L \\ D_3 = G_A(\delta - \delta_0 + \delta_L \xi_0) + E \xi_0(\delta_0 - \delta_L) - \frac{C_1(F - F_0)}{C_2} \\ E = G_A - G_M \end{cases} \quad (8)$$

$$\begin{cases} \xi = \frac{D_2 \pm \sqrt{D_2^2 - 4D_1 D_3}}{2D_1} \\ \xi \in [0,1] \end{cases} \quad (9)$$

According to [12], when the $T > A_s$, memory alloy is in the austenitic process, ξ can be represented by the equation 10, wherein ξ is the temperature of the SMA and C_A is the slope of σ_{cr} (critical stress) over T (curve slope), C_A is measured by experimental data.

$$\begin{cases} \xi = \frac{\xi_0}{2} \left\{ \cos \left[\alpha_A \left(T - A_s - \frac{\sigma}{C_A} \right) \right] \right\} \\ \alpha_A = \pi / (A_f - A_s) \\ \sigma = \sqrt{3} \tau \\ \tau = C_1 F \end{cases} \quad (10)$$

The target temperature TT is available:

$$TT = \frac{\arccos(2\xi/\xi_0 - 1)}{\alpha_A} + A_s + \sigma/C_A \quad (11)$$

Since the voltage signal collected by the temperature sensor is not stable due to the change of ambient temperature and other factors, the Kalman filter algorithm is introduced to obtain relatively stable data.

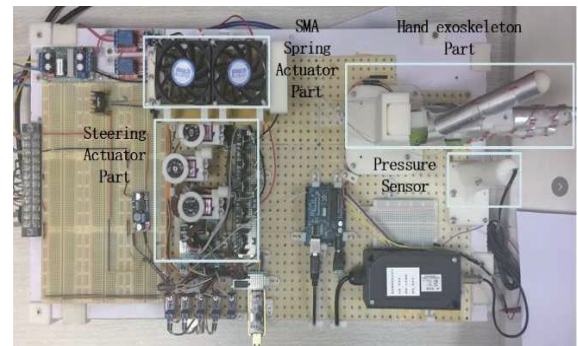


Figure 5. The whole experimental setup

IV. THE SYSTEM ASSESSMENT

A. Experiment setup

In order to verify the effectiveness of the hybrid actuator system and control method, four sets of hand exoskeleton operation experiments were carried out, as shown in Fig. 5. The experimental data, as shown in Table II. The pressure sensor was pre-installed at the target position of the fingertips before the start of the experiment. The target attitude and the target fingertip force are input into the window monitor to obtain the operating temperature and rotation angle of the steering gear required by the SMA spring. According to the target instruction hand exoskeleton actuators to complete the relevant actions. When the system completed the target work, the system immediately stopped heating the alloy spring and turned on the fan for cooling. Each test lasted for 65s, and 8 groups of data were collected, as shown in Fig. 6. The time response experiment of position control was not carried out because the gesture of the finger was actuator by the servomotor winch, which acted very fast, and each movement consumed only sub-second time.

B. Result analysis

Subfigures (a), (c), (e) and (f) of Fig. 6 can reflect the temperature response of the palmar SMA spring, which can reach the target temperature from room temperature within 5 seconds, with a faster response, which can meet the rehabilitation exercise needs of patients.

TABLE II. The ideal data obtained by calculation

Item	Data1	Data2	Data3	Data4
Target Force	2.3N	2.7N	2.3N	2.7N
Target Pose	90°	90°	110°	110°
Target Temp	61.72°C	71°C	52.7°C	60.91°C
SMA Tension	9.46N	11.03N	7.94N	9.27N

Subgraphs (b), (d), (f) and (h) of Fig. 6 show that the output has similar rapid response, and the target force can be reached within 5s. However, because the motion interference of the hand exoskeleton actuator is difficult to avoid in the process of movement, it is more obvious when the exoskeleton is moving at a large Angle.

Therefore, the error of the fingertip output force in subfigures (f) and (h) of Fig. 6 is acceptable. Kalman filter was introduced to denoise fingertip force data, and it was found that the fingertip force changed steadily after fitting, which was in line with the law of human hand movement. During the temperature stabilization process, the fingertip pressure decreases slightly, which is due to the gradual transformation of part of austenite in the SMA material to annealed martensite, which is inevitable on account of the material properties.

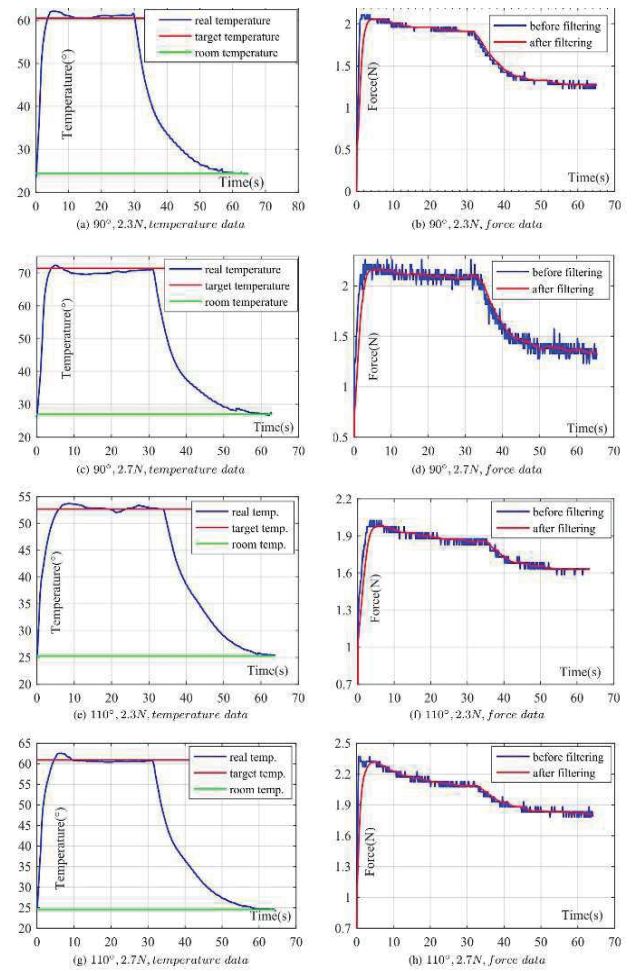


Figure 6. Experimental result

V. CONCLUSION AND FUTURE WORK

In this paper, a novel hybrid actuator designed for coupling tendon actuation is more compact in structure, faster in response, and combines the advantages of servo system and memory alloy actuator. The PID

control algorithm is introduced in the motion control to make the output of SMA spring more stable. The experiment proves that the dynamic system can meet the motion characteristics of the coupling tendon movement. In the future, the actuating mechanism of the hand exoskeleton will be further optimized to reduce motion interference and implement precise force control. Meanwhile, the intelligent perception system of the hand exoskeleton will be designed.

ACKNOWLEDGMENT

This paper was sponsored by the National Natural Science Foundation Grant No. 51505072, and The Fundamental Research Funds for the Central Universities Projects, No. N1601304007, from P.R. China.

REFERENCES

- [1] "Effects of augmented exercise therapy time after stroke: a meta-analysis," *Stroke A Journal of Cerebral Circulation*, 2004.
- [2] M. Cempini, S. M. M. De Rossi, T. Lenzi, N. Vitiello, and M. C. Carrozza, "Self-Alignment Mechanisms for Assistive Wearable Robots: A Kinetostatic Compatibility Method," *IEEE Transactions on Robotics*, vol. 29, no. 1, pp. 236-250, 2013.
- [3] H. Huang, A. Zhu, J. Song, Y. Tu, and Z. Guo, "Characterization and Evaluation of a Cable-Actuated Flexible Hand Exoskeleton *," in *2020 17th International Conference on Ubiquitous Robots (UR)*, 2020.
- [4] Z. MA and P. Ben-Tzvi, "RML Glove—An Exoskeleton Glove Mechanism with Haptics Feedback," *IEEE/ASME Transactions on Mechatronics*, vol. 20, no. 2, pp. 641-652, 2014.
- [5] E. Kaplanoglu, A. E. Cetin, and G. Akgun, "Exoskeleton design and adaptive compliance control for hand rehabilitation," *Transactions of the Institute of Measurement & Control*, vol. 42, no. 3, pp. 493-502, 2020.
- [6] E. Y. Wang and Q. Xu, "Design of a New Soft Robot Hand for Grasping and Sorting Operation," in *2020 10th Institute of Electrical and Electronics Engineers International Conference on Cyber Technology in Automation, Control, and Intelligent Systems (CYBER)*, 2020.
- [7] B. W. K. Ang and C. H. Yeow, "3D Printed Soft Pneumatic Actuators with Intent Sensing for Hand Rehabilitative Exoskeletons*," in *International Conference on Robotics and Automation*, 2019.
- [8] F. Simone, S. Borreggine, G. Rizzello, V. Palmisano, and S. Seelecke, "Modeling and Identification of a Shape Memory Alloy Robotic Finger Actuator," in *2019 European Control Conference (ECC)*, 2019.
- [9] N. Jang et al., "Compact and Lightweight End-Effectors to Actuator Hand-Operated Surgical Instruments for Robot-Assisted Microsurgery," *IEEE/ASME Transactions on Mechatronics*, vol. 25, no. 4, pp. 1933-1943, 2020.
- [10] Xiaobin Feng, "Design and analysis of finger rehabilitation robot driven by shape memory alloy wire," *Yanshan Univ, Qinhuangdao, China*, 2019.
- [11] J. Yang, H. Xie, and J. Shi, "A novel motion-coupling design for a jointless tendon-actuator finger exoskeleton for rehabilitation," *Mechanism & Machine Theory*, vol. 99, pp. 83-102, 2016.
- [12] Brinson and C. L., "One-Dimensional Constitutive Behavior of Shape Memory Alloys: Thermomechanical Derivation with Non-Constant Material Functions and Redefined Martensite Internal Variable," *Journal of Intelligent Material Systems & Structures*, vol. 4, no. 2, pp. 229-242, 1993.